DOI 10.1007/s11595-013-0630-8

Influence of Charge Density and Chain Length on the Interaction between Organic Anion and Montmorillonite

ZHENG Junping, LI Jian, HAO Hui, YAO Kangde

(Tianjin Key Laboratory of Composite and Functional Materials, School of Materials Science and Engineering, Tianjin University, Tianjin 300072, China)

Abstract: Anionic surfactant sodium dodecyl sulfate (SDS), cationic surfactant cetyl trimethyl ammonium bromide (CTAB) and acrylic acid (AA) were introduced as molecular models to study the interaction between montmorillonite and organic molecules with different charge or chain length. The compounds were characterized by X-ray diffraction (XRD), Fourier transform infrared spectroscopy (FT-IR) and ^{13}C nuclear magnetic resonance (^{13}C NMR). The results show organic anion could interact strongly with montmorillonite, even the molecules could intercalate into the layers of MMT.

Key words: chain length; charge density; interaction; montmorillonite.

1 Introduction

By the interaction of cationic surfactants and montmorillonite (MMT), MMT has been applied in colloid chemistry[1], water treatment[2], medical recipients[3-5], and other applications[6]. For the formation of cationic surfactants/MMT compounds, the functional groups of these cationic surfactants can interact with MMT via ion exchange. Also, some factors can influence the interaction process, such as temperature of intercalation system[7], layer charge distribution[8,9], molecular chain length[10-12], size of the surfactant head groups[13], nature of the clay minerals[14], crystallographic and hydration condition.

The interaction between organic anion and MMT has rarely been reported. In these systems, ibuprofen was intercalated into MMT as a sustained release drug carrier[15, 16]. The influence of polyethylene oxides with cationic and anionic groups on the coagulation of sodium montmorillonite dispersions was studied[17]. Billingham *et al* investigated the interaction of polyacrylic acid (PAA) with MMT[18]. In fact, some drug molecules, proteins molecules and other biological molecules are also negatively charged. The objective of this work is to study the interaction mechanism of organic-inorganic substances by analyzing the role of charge density and molecular chain length on the interaction between organic anion and MMT. This provides us with valuable means or information on the separation of proteins, preparation of high-performance compounds, preparation of anionic drugs/MMT compounds and other applications.

2 Experimental

2.1 Materials

MMT (Na^+ MMT) with a cation exchange capacity (CEC) of 90 meq/100 g was provided by Huate Chemical Corp. (Zhejiang, China). CTAB was purchased from Xiangzhong Chemical Reagent Development Center (Hunan, China). SDS was purchased from the Second Plant of Chemical Reagent (Tianjin, China). AA (Tianjin Chemical Reagent Factory, China) was distilled under reduced pressure before use. All other reagents were all of analytical grade.

2.2 Re-crystallization of SDS

SDS (2.19 g) was dissolved in 100 mL de-ionized water and heated at 50 ℃ for 1 h. The emulsion was centrifuged at 4 000 rpm for 30 min. The sediment was dried in a vacuum oven and ground for characterization.

2.3 Re-crystallization of CTAB and SDS mixture

SDS (1.58 g) and CTAB (2.00 g) were dissolved in 100 mL de-ionized water and heated at 50 ℃ for 1

(Received: Oct. 12, 2011; Accepted: Oct. 17, 2012)

ZHENG Junping(郑俊萍): Prof.; Ph D; E-mail: jpzheng@tju.edu.cn

h. Then the mixture was centrifuged at 4 000 rpm for 30 min. The sediment was dried in a vacuum oven and ground for characterization.

2.4 Preparation of CTAB/MMT, SDS/MMT, SDS-CTAB/MMT compounds

Approximately 5 mL (7.5 wt%) CTAB solution (pH=4.0) was added dropwise into 25 mL (3.85 wt%) ultrasonically dispersed MMT suspension under vigorous stirring at 70 ℃ for 1 h. The mixture was centrifuged at 4 000 rpm for 30 min. The sediment was dried in a vacuum oven and ground for characterization.

To prepare the SDS-CTAB/MMT and SDS-CTAB/MMT samples, about 5 mL (10 wt %) SDS solution or a certain amounts SDS-CTAB (molar ratio 1:1) compounds were added dropwise into the same MMT suspension, respectively. The mixtures were treated as mentioned above to prepare SDS/MMT and SDS-CTAB/MMT compounds.

2.5 Preparation of SDS/CTAB/MMT compound

Approximately 2.8 mL (10 wt%) SDS solution was dissolved in 25 mL CTAB/MMT suspension. The mixture was treated with the same procedures described for the preparation of SDS/MMT.

2.6 Preparation of AA/MMT compounds and PAA/MM compounds at different pH

Various pH of AA solutions (50 wt%, pH=1.6, 3.0 and 9.0) or PAA solutions (50 wt%, pH=1.7 and 4.0) were added dropwise into 25 mL (3.85 wt%) ultrasonically dispersed MMT suspensions under vigorous stirring at 70 ℃ for 1 h. The mixture was centrifuged at 4 000 rpm for 30 min. The sediment was dried in a vacuum oven and ground for characterization.

2.7 Characterization

X-ray diffraction (XRD) patterns were recorded at 4 °/min on a Japan Rigaku DMAX-RC diffractometer by using CuKα radiation at a generator voltage of 40 kV and a generator current of 100 mA. The FT-IR spectra of the samples were taken with a BIO-RAD FTS3000 FT-IR spectrophotometer using KBr pellets in the range of 4 000-400 cm^{-1}. The solid state ^{13}C NMR CP/MAS measurements were performed on an OXFORD Infinity plus 300WB spectrometer operating at a spinning frequency of 3 kHz. The 90° pulse time used in high proton-de-coupled single pulse ^{13}C spectra was 4.5 μs and pulse delay was 5.0 s. The spectrum width was 40 kHz.

3 Results and discussion

3.1 Effect of charge density

The XRD patterns of MMT, CTAB/MMT and SDS/MMT are shown in Fig.1. Pristine MMT exhibits a sharp peak at 2θ=7.04º, corresponding to a basal spacing of 1.25 nm. The peak at 2θ=2.94º (d_{001}=3.00 nm) can be observed in the XRD pattern of CTAB/MMT, suggesting that CTAB intercalates into MMT through the ion exchange reaction. For SDS/MMT, there is still a sharp peak at 2θ=7.04º, which is the d_{001} characteristic peak of MMT. But there are still two peaks at lower angles. As the compound contains only two substances-MMT and SDS, the diffraction peaks at lower angles belong to re-crystallization of SDS.

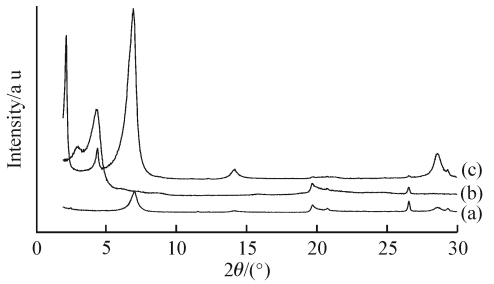

Fig.1 XRD patterns of (a) MMT; (b) CTAB/MMT; and (c) SDS/MMT

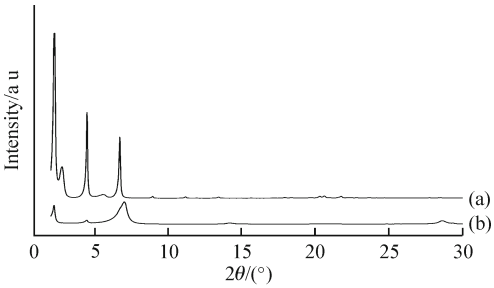

Fig.2 XRD patterns of (a) SDS/MMT and (b) re-crystallization of SDS

The XRD patterns of SDS/MMT and re-crystallization of SDS are shown in Fig.2. By comparison, the diffraction peaks at low angles (2θ=2.24º and 4.46º) of SDS/MMT are characteristic diffraction peaks of re-crystallization of SDS, confirming the former speculation. In the XRD pattern of SDS/MMT, the peak at about 7° may be the superposition of the peak of re-crystallization of SDS and the peak of MMT. The result reveals that SDS molecular chains can not intercalate into the layers of MMT, due to the large negative charge density, which can generate very strong charge repulsion.

The FT-IR spectra of SDS, SDS/MMT and MMT are shown in Fig.3. The characteristic vibration bands of MMT are shown at 3 626 cm^{-1} (—OH stretch from Al—OH), 3 400 cm^{-1} (—OH stretch from free H_2O), 1 639 cm^{-1} (—OH deformation of water), 1 421 cm^{-1}

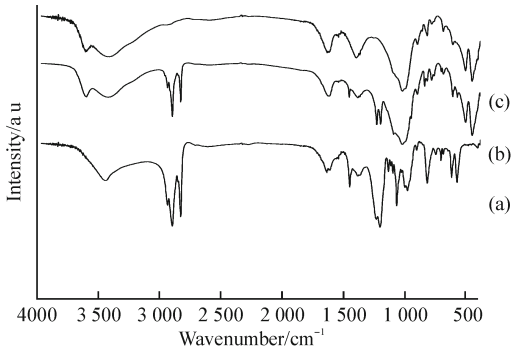

Fig.3 FT-IR spectra of (a) SDS; (b) SDS/MMT; and (c) MMT

(asymmetric stretch of CO_3^{2-} ion), 1 034 cm^{-1} (Si—O stretch), 914 cm^{-1} (AlAlOH deformation), and 520 cm^{-1} and 500 cm^{-1} (Si—O stretch).[19, 20] Those of SDS are shown at 2 923 and 2 850 cm^{-1}(–CH_3 and –CH_2– stretch), 1 390 cm^{-1}(anti-symmetric stretch of SO_2), 1 200 cm^{-1} (symmetric stretch of SO_2), and 980 and 820 cm^{-1} (anti-symmetric stretch of O—S—O). In the spectrum of SDS/MMT, the characteristic peaks of SDS and MMT can be recognized easily, suggesting the formation of the blend. In particular, the characteristic absorption peak of SDS at 1 200 cm^{-1} in the spectrum of SDS/MMT splits at 1 215 cm^{-1} and 1 250 cm^{-1} obviously. This result reveals the interaction of –SO_4^{2-} and MMT.

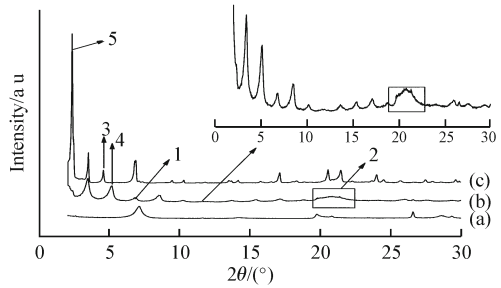

Fig.4 XRD patterns of (a) MMT; (b) SDS-CTAB/MMT; and (c) Re-crystallization of SDS-CTAB

The XRD patterns of MMT, SDS-CTAB/MMT and re-crystallization of SDS-CTAB are shown in Fig.4. For SDS-CTAB/MMT, there is still a peak (Fig.4(b), 1) which corresponds to the characteristic d_{001} peak of MMT (2θ=7.04º), however, the relative intensities of this peak and the other characteristic peaks at 20-22º (Fig.4(b), 2) are weaker than those of MMT (Fig.4(a)) in the same position. Also, there are two sharp peaks (2θ=3.42º and 5.14º) which is to the left of peak 1. The phenomenon indicates that peak 1 may be re-crystallization peak of SDS-CTAB. Comparing the XRD patterns of SDS-CTAB/MMT and re-crystallization of SDS-CTAB, the peak at 7.04º (Fig.4(b)) is not the characteristic peak of MMT. The peaks appearing at low angles between 2º and 7.04º except peak 4 (2θ=5.12º) correspond well to the crystallization peaks of the re-crystallization of SDS-CTAB (Fig.4(c)). When SDS-CTAB interacts with MMT, MMT affects the crystal structure of the organic compounds, leading to peak 3 shifting from 4.52º to 5.12º and the d_{001} peak of MMT shifting toward lower angle value. This phenomenon indicates that peak 3 and peak 4 are the same diffraction peaks of crystal structure. Moreover, comparing the magnified XRD patterns of SDS-CTAB/MMT, peak 5 of re-crystallization of SDS-CTAB with the lowest 2θ value (2.3º) and the largest intensity, is weakened obviously in the XRD pattern of SDS-CTAB/MMT. This observation suggests that peak 4 is not the characteristic d_{001} peak of MMT.

As there is no peak in the left side of peak 5 (2.3º) in the pattern of SDS-CTAB/MMT, the characteristic d_{001} peak of MMT disappears. This means the interaction between SDS-CTAB and MMT is relatively strong, the molecules intercalate into interlayers of MMT, and ordered structure has been destroyed even forming the exfoliation structure. It can be explained that the addition of CTAB into SDS decreases the negative charge density and charge repulsion.

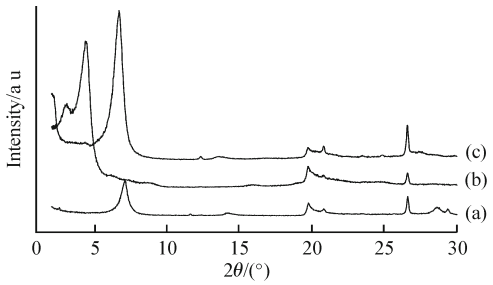

Fig.5 XRD patterns of (a) MMT; (b) CTAB/MMT; and (c) SDS/CTAB/MMT

The XRD patterns of MMT, CTAB/MMT and SDS/CTAB/MMT are shown in Fig.5. When SDS was added into the solution of CTAB/MMT compound, the d_{001} peak of SDS/CTAB/MMT shifts from 2.94º of CTAB/MMT to 6.66º and interlayer spacing decreases from 3.00 nm to 1.33 nm, which is similar to the d_{001} of pristine MMT. This phenomenon indicates that the de-intercalation of CTAB/MMT occurs after the addition of SDS and the interactive intensity between SO_4^{2-} and $-NH_4^+$ is stronger than that between MMT and $-NH_4^+$.

3.2 Effect of chain length

According to our previous work[21], sodium laurate molecule could not intercalate into MMT due to the strong charge repulsion between anionic charges of sodium laurate and anionic charges on the sheets of MMT. In fact, molecular chain length may be a fact influencing the interaction and intercalation. In this

paper, AA was chosen to study the interaction between —COO– and MMT, due to its short alkyl chain (only three C atoms) and small steric hindrance.

3.2.1 Interaction of AA and MMT

Table 1 XRD data of MMT and AA/MMT prepared at different pH

pH	2θ/(°)	d_{001}/nm
	7.04	1.25
1.6	5.38	1.64
3.0	5.30	1.67
9.0	4.46	1.98

AA exhibits different molecular structure at different pH, and when pH <1.7, the carboxylic acid groups exist mainly in —COOH; when pH> 1.7, it exist mainly in —COO^-. The XRD patterns of MMT and AA/MMT prepared at different pH are shown in Fig.6. The d_{001} data of MMT and AA/MMT are listed in Table 1. AA molecules successfully intercalated into MMT, no matter in acidic or alkaline medium. This phenomenon indicates that the carboxylic anion (—COO^-) and the carboxyl (—COOH) can both interact strongly with MMT. As can be seen from Table 1, pH obviously affects the intercalation effect. The interlayer spacings of AA/MMT compounds prepared at pH of 1.6 and 3.0 are almost the same. When AA/MMT was prepared at pH=9.0, the interlayer spacing can nearly reach to 2.00 nm, obviously different from the formers. The peak at 7.82º (Fig.6(d)) may be re-crystallization peak of free AANa. These phenomena indicated that the arrangement of AA molecules between the MMT layers in alkaline medium is completely different from that in acidic medium.

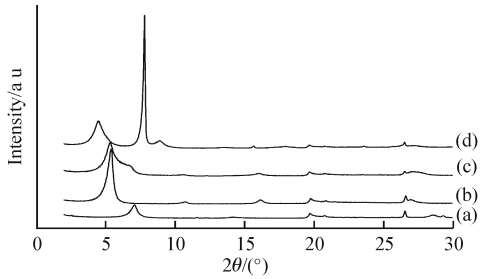

Fig.6 XRD patterns of MMT and AA/MMT prepared at different pH: (a) MMT and (b)AA/MMT composites at pH of 1.6 ; (c) pH3.0; and (d) pH 9.0

In many cases, the intercalated molecules are known to align themselves in an ordered structure within the interlayer space[22-24]. The structure model of AA/MMT at pH of 1.6 is shown in Fig.7(a). In acidic medium, carboxylic acid group is in the form of —COOH, which is generally considered as carrying no charge. When AA interacts with MMT, AA molecules intercalate into interlayers of MMT as neutral structure, therefore, the molecules tend to be in single arrangement. When water molecules between the MMT interlayers are removed by heating in a vacuum oven, the interlayer spacing becomes about 1 nm[25]. As pH is 9.0, the interlayer spacing of AA/MMT increases from 1 nm to 2.0 nm. In this case, carboxylic acid group of AANa mainly exists in the form of —COO^-, and AANa molecules in the MMT layers are double-layer structure arrangement (Fig.7(b)). When AANa molecules intercalate into interlayers of MMT, negative charge density between layers increases, then inter-lamellar repulsion increases and inclines to double-layer arrangement.

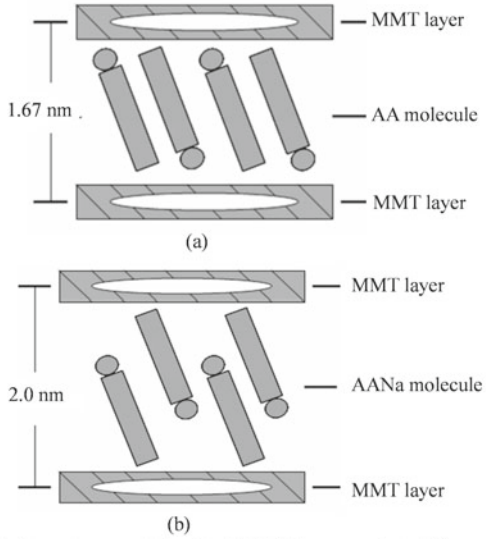

Fig.7 Structure models of AA/MMT prepared at different pH: (a) AA/MMT at pH of 1.6 and (b) pH 9.0

The FT-IR spectra of MMT, AANa and AANa/MMT(prepared at pH=9.0) are shown in Fig.8. The spectrum of AANa/MMT displays both the characteristic bands at 1 560 cm^{-1} (—COO^- stretching vibration) of AANa and the absorbances at 3 626 cm^{-1} (Al—OH stretching vibration) and 1 034 cm^{-1} (Si—O stretching vibration) of MMT, therefore, the formation of AANa/MMT compound was confirmed. And the peak at 1 721 cm^{-1} (—C=O stretching vibration) of the AANa disappears in the spectrum of AANa/MMT, maybe due to the interaction between AANa and MMT.

The ^{13}C NMR spectrum of AANa/MMT (prepared at pH=9.0) is shown in Fig.9. ^{13}C NMR data of AA are listed in Table 2. Generally speaking, for the carboxylate, chemical shift of C atom of —COO^- is about 5 ppm larger than that of —COOH. Then, chemical shift of the carbon atom in —COO^- of AANa should be about 177 ppm. In the ^{13}C NMR spectrum

of AANa, the signals at 175.7, 140.3 and 123.2 ppm are assigned to C1, C2 and C3 of AANa respectively. However, there is another resonance hump of C1 in 182.3 ppm, splitting into three humps (chemical shift are 183.5, 182.3, and 179.5, respectively). This phenomenon indicates that the chemical environment of the carbon atoms greatly changes, due to the interaction between —COO^- and MMT.

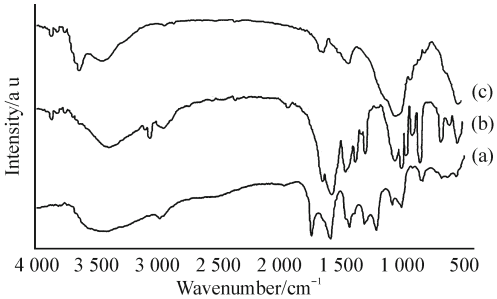

Fig.8 FT-IR spectra of (a) AANa; (b) AANa/MMT; and (c) MMT

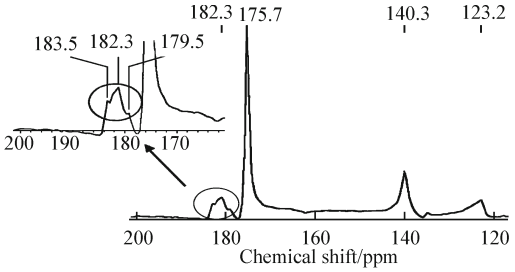

Fig.9 Solid state ^{13}C NMR spectrum of AANa/MMT

Table 2 ^{13}C NMR data of AA

Carbon number	Chemical shift/ppm	Molecular formula
1	171.95	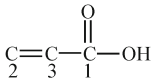
2	133.15	
3	128.14	

When organic anion with carboxyl functional group interacts with MMT, the interactive sites is the carboxyl group (—C=O) and hydroxyl group (—OH) is the interactive site on MMT sheets[21]. In this study, —C=O of organic anion may interact with the aluminium hydroxyl group (Al-OH) or the aluminium ion (Al^{3+}) of MMT.

3.2.2 Interaction of PAA /MMT at different pH

Fig.10 shows the XRD patterns of the PAA / MMT prepared at different pH. The interlayer spacing of PAA/MMT prepared at pH = 1.7 is 1.77 nm, suggesting that PAA interacts with MMT, and PAA molecular chains intercalate into interlayers of MMT. When adjusting pH value to 4.0, the interlayer spacing (d_{001}=1.31 nm) is almost the same as that of the pristine

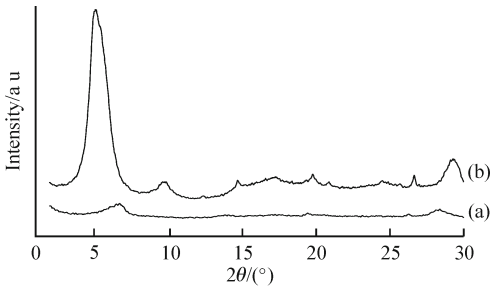

Fig.10 XRD patterns of the PAA /MMT prepared at different pH: PAA/MMT composites at pH of (a) 4.0 and (b) 1.7

MMT (d_{001}=1.25 nm).

Carboxylic acid group (—COOH) of PAA at low pH is electroneutral while at high pH electronegative. When at high pH, the density of —COO^- is relatively high, similar to that of AANa. Due to the long molecular chains of PAA, steric hindrance and negative charge repulsion cause the interaction resistance between PAA and MMT. The interaction can not be realized. In contrast, in low pH value, the density of —COO^- is relatively low. Despite the chain length of PAA is large, due to the charge repulsion decrease, the interaction force between —COOH and MMT is greater than that of steric hindrance.

4 Conclusions

AA and SDS were introduced as molecular models to investigate the interaction between organic anion and MMT. It is found that SDS molecules with anionic charge could not intercalate into the layers of MMT due to the large negative charge density. Whereas, SDS molecule treated by CTAB leading to the relative decrease of negative charge density, could interact with MMT strongly, even the molecular chains could intercalate into the layers of MMT. For PAA molecules and AA molecules, —COOH and —COO^- could interact with MMT, however, due to the fact that PAA molecular chain length is relatively large, PAA at high pH could not intercalate into the layers of MMT. When at low pH, the density of —COO^- of PAA/MMT decrease, and PAA can interact with MMT strongly. It is ascertained that organic anion can also interact strongly with MMT, even the molecules can intercalate into the layers of MMT. The interaction depends on charge density and molecular chain length.

References

[1] Janek M, Lagaly G. Interaction of a Cationic Surfactant with Bentonite: a Colloid Chemistry Study [J]. *Colloid. Polym. Sci*., 2003, 281: 293-301

[2] Morris R J, Williams D E, Luu H A, *et al*. The Adsorption of Microcystin-LR by Natural Clay Particles [J]. *Toxicon*, 2000, 38: 303-308

[3] Lin F H, Lee Y H, Wang J M, *et al*. A Study of Purified Montmorillonite Intercalated with 5-Fuorouracil as Drug Carrier[J]. *Biomaterials,* 2002, 23: 1 981-1 987

[4] Shi Q S, Tan S Z, Yang Q H, *et al*. Preparation and Characterization of Antibacterial Zn^{2+}-Exchanged Montmorillonites [J]. *J. Wuhan University of Tech. -Mater. Sci. Ed*., 2010, 25(5): 725-729

[5] Meng N, Zhou N L, Zhang S Q, *et al*. Synthesis and Antifungal Activities of Polymer/Montmorillonite–Terbinafine Hydrochloride Nanocomposite Films[J]. *App. Clay Sci*., 2009, 46: 136-140

[6] Wan T, Xu H H, Yuan Y, *et al*. Preparation and Photochemical Behavior of a Cationic Azobenzene Dye-Montmorillonite Intercalation Compound [J]. *J. Wuhan University of Tech. -Mater. Sci.Ed*., 2007, 22(3): 466-469

[7] Joshi G V, Patel H A, Kevadiya B D, *et al*. Montmorillonite Intercalated with Vitamin B1 as Drug Carrier [J]. *App. Clay Sci*., 2009, 45: 248-253

[8] Lee S Y, Cho W J, Hahn P S, *et al*. Microstructural Changes of Reference Montmorillonites by Cationic Surfactants [J]. *App. Clay Sci*., 2005, 30: 174-180

[9] Pálková H, Madejová J, Komadel P. The Effect of Layer Charge and Exchangeable Cations on Sorption of Biphenyl on Montmorillonites[J]. *Cent. Eur. J. Chem*., 2009, 7: 494-504

[10] Cenens J, Shoonheydt R A. Visible Spectroscopy of Methylene Blue on Hectorite, Laponite B, and Barasym in Aqueous Suspension [J]. *Clays Clay Miner.*, 1988, 36: 214-224

[11] Fejér I, Kata M, Erös I, *et al.* Interaction of Monovalent Cationic Drugs with Montmorillonite[J]. *Colloid. Polym. Sci.*, 2002, 280: 372-379

[12] Fejér I, Kata M, Erös I, *et al.* Release of Cationic Drugs from Loaded Clay Minerals [J]. *Colloid. Polym. Sci*., 2001, 279:1 177-1 182

[13] Imai Y, Nishimura S, Inukai Y, *et al.* Differences in Quasicrystals of Smectite-Cationic Surfactant Complexes Due to Head Group Structure [J]. *Clays Clay Miner*., 2003, 51: 162-167

[14] Lagaly G, Beneke K. Intercalation and Exchange-reactions of Clay-minerals and Non-clay Layer Compounds[J]. *Colloid. Polym. Sci.*, 1991, 269: 1 198-1 211

[15] Zheng J P, Luan L, Wang H Y, *et al*. Study on Ibuprofen/ Montmorillonite Intercalation Composites as Drug Release System [J]. *App. Clay Sci*., 2007, 36: 297-301

[16] Zheng J P, Wang H Y, Zhuang H, *et al.* Intercalation of Amido Cationic Drug with Montmorillonite[J]. *J. Wuhan University of Tech. -Mater. Sci. Ed.*, 2007, 22 (2): 250-252

[17] Lagaly G, Ziesmer K. Colloid Chemistry of Clay Minerals: the Coagulation of Montmorillonite Dispersions [J]. *Adv. Colloid Interface Sci*., 2002, 100-102: 105-128

[18] Billingham J, Breen C, Yarwood J, *et al.* Adsorption of Polyamine, Polyacrylic Acid and Polyethylene Glycol on Montmorillonite: An *in situ* Study Using ATR-FTIR [J]. *Vib. Spectrosc.*, 1997, 14: 19-34

[19] Farmer V C. *The Infrared Spectra of Minerals*[M]. London: Mineralogical Society, 1974

[20] Madejová J, Komadel P. Baseline Studies of the Clay Minerals Society Source Clays: Infrared Methods[J]. *Clays Clay Miner*., 2001, 49: 410-432

[21] Xu S W, Zheng J P, Tong L, *et al.* Interaction of Functional Groups of Gelatin and Montmorillonite in Nanocomposite[J]. *J. Appl. Polym. Sci*., 2006, 101: 1 556-1 561

[22] Lagaly G. Layer Charge Determination by Alkylammonium Ions. In: A.R. Mermut, Editor. Layer Charge Characteristics of 2:1 Silicate Clay Minerals[R]. *CMS Workshop Lectures,* The Clay Minerals Society, 1994

[23] Sposito G, Prost R. Structure of Water Adsorbed on Smectites [J]. *Chem. Rev.*, 1982, 82: 553-573

[24] Ogawa M, Kuroda K. Photofunctions of Intercalation Compounds [J]. *Chem. Rev.*, 1995, 95: 399-438

[25] Karabomi S, Smit B, Heidug W. The Swelling of Clay: Molecular Simulations of the Hydration of Montmorillonite[J]. *Science*, 1996, 271: 1 102-1 104